In vivo T1ρ mapping in cartilage using 3D Magnetization-prepared Angle-modulated Partitioned-k-space Spoiled gradient echo Snapshots (3D MAPSS)

X. Li[1], E. T. Han[2], R. F. Busse[3], and S. Majumdar[1]

[1]Musculoskeletal Quantitative Research (MQIR), Department of Radiology, University of California at San Francisco, San Francisco, CA, United States, [2]Global Applied Science Lab, GE Healthcare, Menlo Park, CA, United States, [3]Global Applied Science Lab, GE Healthcare, Wisconsin, United States

INTRODUCTION Non-invasive methods for the early detection of cartilage degeneration in osteoarthritis (OA) are of increasing clinical importance. $T_{1\rho}$ describes the spin-lattice relaxation in the rotating frame and has been proposed as an attractive candidate to probe changes in the extracellular matrix of cartilage during the early stages of OA [1-3]. For $T_{1\rho}$ quantitation, a 3D acquisition is desired in order to obtain high-resolution images and consequently an accurate assessment of cartilage degeneration. Current 3D methods that use steady state spoiled gradient echo imaging suffer from high SAR, low SNR and the need for retrospective correction of contaminating T1 effects [2]. Based on our previous work [4], a novel 3D acquisition scheme - 3D **M**agnetization-prepared **A**ngle-modulated **P**artitioned-k-space **S**poiled Gradient Echo **S**napshots (3D MAPSS) – was developed and used to obtain *in vivo* $T_{1\rho}$ maps.

MATERIALS AND METHODS *Theory and simulation* The $T_{1\rho}$-weighted imaging sequence is composed of two parts: magnetization preparation for $T_{1\rho}$ pre-encoding, and a 3D SPGR acquisition during transient signal evolution immediately after mag prep (Fig. 1). All acquisitions experience the same amount of saturation recovery after mag reset (T_{rec}). The spin-lock pulse cluster consists of a hard 90^0 pulse followed by a spin-lock pulse (with duration time of spin lock, TSL) and a hard -90^0 pulse. Multiple k-space lines (views per segmentation, VPS) are acquired after each mag prep, traversing segmented elliptic-centric order. The transverse magnetization after the *nth* α pulse can be described as $M_{xy}(n)=A(n)M_{prep}+B(n)$, where $B(n)$ relates to longitudinal relaxation that adversely affects the accuracy of quantification if uncorrected [5]. In addition, signal evolution during the transient stage imposes different weights to each phase encoding step, acting as a k-space filter whose characteristics depends on M_{prep}, T_1, TR and flip angle. To eliminate the $B(n)$ term, an RF chopping scheme was used. Two acquisitions, one with a –90 after spin lock and the other with a +90, are subtracted, the latter from the first. This RF chopping scheme also yields a transient signal evolution that is independent of M_{prep}. A flip angle train was then designed based on simulation of an iterative Bloch equation to provide a flat signal response [6]. To maximize SNR, the last flip angle was constrained to be 90^0. Fig 2 illustrates signal evolution during the α train for acquisitions (a) without RF chopping ('nochop') and (b) with RF chopping ('chop') and RF chopping + optimized flip angle (MAPSS). Fig 2c shows the resulting $T_{1\rho}$ fits. Simulation parameters: TR=9.3ms, T_{rec}=1500ms, VPS=64, TSL=0,10,40,80ms, T_1=1240ms and $T_{1\rho}$=45ms. *Phantom and in vivo imaging* All data were acquired at a 3T GE EXCITE scanner (Waukesha, WI) using a quadrature knee coil. A T_1 phantom (T_1 = 950 ms at 3T) and phantoms with different concentration of agerose (2% and 4%) were scanned using TR/TE = 9.3/min full; FOV = 10 cm, matrix = 256 * 128, slice thickness = 4mm, BW=31.25kHz, VPS = 64, T_{rec}=500ms, TSL = 0,10,40,80ms, f_{SL}=500 Hz. The phantom with 4% Agar was imaged six times at different locations with repositioning between scans. Four healthy volunteers (2 female, 2 male, age range = 19 – 34 years) without any clinical symptoms of OA or other knee injuries were scanned twice with repositioning between scans using the same parameters but with a FOV=14cm and T_{rec}=1500ms. The $T_{1\rho}$ map was reconstructed by fitting the $T_{1\rho}$-weighted images $S(TSL) \propto \exp(-TSL/T_{1\rho})$. The fitting goodness was evaluated using normalized fitting errors defined as $sqrt[sum(y-y_{fit})^2/(n-1)]/SD$, where n=4 is the number of TSL. Nine regions of cartilage, lateral femoral condyle (LFC, further dividing into weight-bearing (wb), non-wb anterior and non-wb posterior), medial femoral condyle (MFC, wb, nwb ant, nwb post), lateral tibia (LT), medial tibia (MT) and patellar were segmented semi-automatically using high-resolution SPGR images. Mean and SD of $T_{1\rho}$ values and fitting errors were studied in each of these compartments. The global and regional reproducibility were estimated with coefficients of variation (CV, SD/mean).

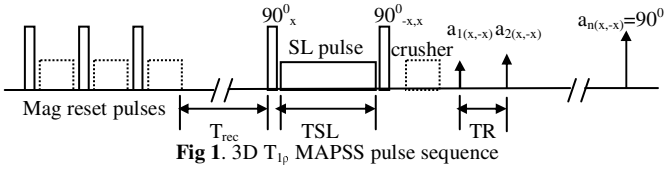

Fig 1. 3D $T_{1\rho}$ MAPSS pulse sequence

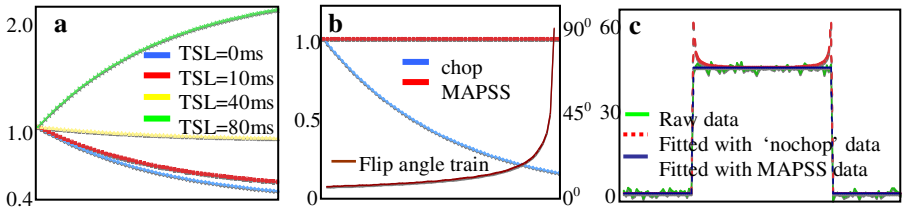

Fig 2. Signal evolution (normalized to signal after 1st α pulse) using nochop seq (a), chop and MAPSS seq (b) and flip angle train used in MAPSS seq (b). (c) Fitted values with nochop and MAPSS seqs.

RESULTS Fig 3 shows the $T_{1\rho}$-weighted images for the T1 phantom using 'nochop' and MAPSS respectively. Significant edge enhancement is shown in the $T_{1\rho}$-weighted images with TSL = 40 ms and 80 ms using 'nochop.' No such effects are seen in the images acquired using MAPSS. The $T_{1\rho}$ values are 48.9 ± 6.4 ms and 86.5 ± 10.0 ms for 4% and 2% Agar phantoms respectively, consistent with our previous results. The CV for the mean $T_{1\rho}$ for the 4% phantom is 0.9%. Table 1 shows the mean, SD and average CV of $T_{1\rho}$ values using MAPSS. The average CV for mean $T_{1\rho}$ in overall cartilage (global reproducibility) is 1.6%. Regional reproducibility varies between 1.7% and 6.4%. Fig 4 (a) and (b) are the fitted $T_{1\rho}$ maps using MAPSS and 'no chop' sequences respectively. $T_{1\rho}$ values are artificially elevated at the edge of LFC (arrow) in the map with 'no chop'. Fig 5 shows that the fitting error using MAPSS are significantly lower ($P < 0.05$) than using 'nochop' seq.

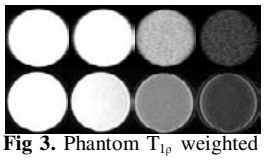

Fig 3. Phantom $T_{1\rho}$ weighted images using MAPSS (upper) and 'nochop' (lower).

Table 1. Average $T_{1\rho}$ and CV for overall cartilage and in each compartment using MAPSS

	Overall	LFC			MFC			LT	MT	Patella
		nwb-ant	nwb-post	wb	nwb_ant	nwb_post	wb			
$T_{1\rho}$(ms)	42.4±5.2	45.0±6.8	41.9±4.2	41.1±3.7	43.8±6.1	42.9±4.0	41.2±1.5	36.8±3.2	40.7±4.2	43.2±1.3
CV	1.6%	6.0%	1.7%	6.4%	8.7%	4.8%	6.4%	3.0%	5.8%	4.1%

CONCLUSIONS AND DISCUSSION A reproducible *in vivo* 3D $T_{1\rho}$ mapping sequence based on MAPSS was developed. By acquiring more than one view per spin lock pulse, the MAPSS sequence has a lower SAR and higher SNR efficiency than the current steady state 3D method [2]. In addition, RF chopping eliminates T1 contamination of the resulting fits and also results in the same filtering effect independent of TSL. This later fact makes it possible to correct for k-space filtering effects by using the same modulated flip angle train when acquiring $T_{1\rho}$-weighted images with different TSLs. Simulation shows that shorter VPS generates higher flip angles in MAPSS sequence and provides higher SNR efficiency. VPS=64 was used to obtain a practical acquisition time of approximately 15 minutes (4 TSLs). Using parallel imaging will help to reduce scan time to a more clinically acceptable duration. Currently under development is a 3D T2 MAPSS sequence which will be used in combination with 3D $T_{1\rho}$ MAPSS to assess and characterize cartilage degeneration.

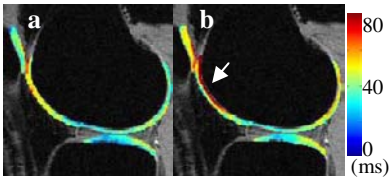

Fig 4. $T_{1\rho}$ maps using MAPSS (a) and 'nochop' (b). Artificially high $T_{1\rho}$ was seen (arrow) in the 'nochop' image.

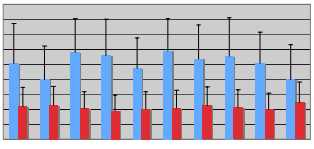

Fig 5. Fitting error (normalized to noise SD) using 'nochop' (blue) and MAPSS (red) respectively in overall cartilage and the nine compartments (same order in table 1)

REFERENCES 1. Duvvuri, U, et al., MRM, 1997. 38(6): 863-7. 2. Regatte RR, et al., Acad Radiol 2004. 11(7):741-9. 3.Li X, et al, MRM 2005, 54(4): 929-36. 4. Han E, et al, ISMRM 2005. 5. Coremans J, JMR 1997 124, 323-42. 6. Mugler et al., MRM 1992, 28:165-85.

ACKNOWLEDGEMENT This research was supported by NIH K25 AR053633 and RO1 AR46905.